0026-895X/97/040637-07$3.00/0

MOLECULAR PHARMACOLOGY, **51:**637–643 (1997).

# Predominant Expression of Monoamine Oxidase B Isoform in Rabbit Renal Proximal Tubule: Regulation By $I_2$ Imidazoline Ligands in Intact Cells

C. GARGALIDIS-MOUDANOS, A. REMAURY, N. PIZZINAT, and A. PARINI

*Institut National de la Santé et de la Recherche Médicale U388, Institut Louis Bugnard, Centre Hospitalier Universitaire Rangueil, 31403 Toulouse Cedex 04, France*

Received September 19, 1996; Accepted December 30, 1996

**SUMMARY**

Previous studies have shown that a subpopulation of the catecholamine-degrading enzymes monoamine oxidase (MAO) A and B holds a previously unknown regulatory site, the $I_2$-imidazoline binding site ($I_2$BS). In the present work, we characterized the isoforms of monoamine oxidases expressed in the rabbit renal proximal tubule, defined their relationship with $I_2$BS, and investigated the ability of $I_2$BS ligands to inhibit enzyme activity in intact cells. Two findings indicate that MAO-B is the predominant isoform expressed in the renal proximal tubule cells: 1) Western blot performed with an anti–MAO-A/MAO-B polyclonal antiserum revealed a single 55-kDa band corresponding to MAO-B; 2) enzyme assays showed an elevated MAO-B activity ([$^{14}$C]$\beta$-phenylethylamine oxidation: $V_{max}$ = 1.31 ± 0.41 nmol/min/mg protein), whereas MAO-A activity was only detectable ([$^{14}$C]5-HT oxidation: $V_{max}$ = 80.3 ± 19 pmol/min/mg protein). Photoaffinity labeling with the $I_2$BS ligand [$^{125}$I]2-(3-azido-4-iodophenoxy)-methylimidazoline revealed a single 55-kDa band, which indicates that MAO-B of the renal proximal tubule cells holds the $I_2$ imidazoline binding site. [$^3$H]Idazoxan binding studies and enzyme assays showed that, in intact cells, $I_2$BS ligands bind to and inhibit MAO-B. Indeed, the increase in the accessibility of intracellular compartment by cell permeabilization did not enhance [$^3$H]idazoxan binding, which indicates that, in intact cells, intracellular $I_2$BS are fully occupied by imidazoline ligands. In addition, enzyme assays showed that incubation of proximal tubule cells with imidazoline ligands leads to a complete, dose-dependent inhibition of MAO activity. These data show the predominant expression of MAO-B in rabbit renal proximal tubule and its regulation by imidazoline ligands in intact cells.

MAO (EC 1.4.3.4) are mitochondrial enzymes involved in the oxidative deamination of neurotransmitters (i.e., norepinephrine, dopamine, and 5-HT) and exogenous amines (1). They participate in the control of cell functions through different mechanisms, including the regulation of neurotransmitter concentrations, the generation of oxygen reactive species, and the production of active metabolites. Two isoforms of the enzyme, MAO-A and MAO-B, have been identified. They are encoded by two distinct genes with an intron/exon structure (2, 3) and can be differentiated based on the substrate specificity and the inhibition by synthetic compounds (1, 4). MAO-A preferentially metabolizes 5-HT and is inhibited by clorgyline and RO 41–1049; MAO-B has a greater affinity for phenylethylamine and is selectively inhibited by deprenyl and RO 19–6327. Both isoforms display similar affinities for dopamine, adrenaline, and noradrenaline (1, 5). Several studies have shown that each of the two isoforms is specifically altered in different pathologies: a decrease in MAO-A activity is associated with aggressive behavior in humans and transgenic mice (6, 7); on the other hand, MAO-B seems to play a critical role in the development and/or maintenance of some neurodegenerative disorders, such as the Parkinson's and Alzheimer's diseases (8–11).

Recently, we identified a previously unknown MAO regulatory site, $I_2$BS, and showed its localization on both MAO-A and MAO-B (12, 13). This binding site, the major characteristic of which is its high affinity for a series of imidazoline and guanidinium compounds, is distinct from the catalytic site (12), the FAD prosthetic group (14) and the binding sites of classical MAO inhibitors (13, 15). The identification of $I_2$BS has provided evidence for the existence of a heterogeneous population of MAO-B. Indeed, photoaffinity labeling using [$^{125}$I]AZIPI showed that $I_2$BS could be identified on

This work was supported by Institut National de la Santé et de la Recherche Médicale, the Region Midi-Pyrénées, and I.R.I. Servier (France). C.G.-M. is the recipient of a grant from the Alexander S. Onassis Foundation.

**ABBREVIATIONS:** MAO, monoamine oxidase(s); AZIPI, 2-(3-azido-4-iodophenoxy)-methylimidazoline; $I_2$BS, $I_2$-imidazoline binding site; HEPES, 4-(2-hydroxyethyl)-1-piperazineethanesulfonic acid; LDH, lactate dehydrogenase; SDS, sodium dodecyl sulfate; PAGE, polyacrylamide gel electrophoresis; 5-HT, 5-hydroxytryptamine (serotonin); PEA, $\beta$-phenylethylamine; EGTA, ethylene glycol bis($\beta$-aminoethyl ether)-*N*,*N*,*N*′,*N*′-tetraacetic acid.

human liver but not on human platelet MAO-B (13). This finding is particularly interesting; it suggests that $I_2$BS may represent the first target for the identification and the pharmacological control of a specific subpopulation of the enzyme. The functional relevance of $I_2$BS has been supported by enzyme assays, which show that, in membrane preparations from rabbit kidney (12), rat liver, and adipocytes (15), MAO activity is inhibited by selective $I_2$BS ligands in a noncompetitive manner. Although these results suggest that $I_2$BS ligands may represent a new class of MAO inhibitors, it was still necessary to show that these molecules are able to diffuse into the cells to interact with mitochondrial MAO.

Among the organs, the kidney displays one of the highest MAO activities. Both MAO-A and MAO-B have been identified in the cortex and medulla of rat and human kidney: MAO-B is predominant in the renal cortex, whereas MAO-A seems to be equally expressed in the cortex and the medulla (16).

Three findings suggest that MAO may have a particularly important role in the renal proximal tubule: 1) the MAO substrates norepinephrine, 5-HT, and dopamine play a critical role in renal proximal tubule sodium reabsorption (17–19); 2) dopamine can be directly produced and secreted by the proximal tubule (20, 21); and 3) dopamine release and metabolism by rat renal cortical slices depend, in part, on the degree of MAO activity (22).

In the present work, we characterized the isoforms of MAO expressed in the rabbit renal proximal tubule, defined their relationship with $I_2$BS, and investigated the ability of $I_2$BS ligands to inhibit enzyme activity in intact cells.

Our results show that MAO-B is the predominant isoform expressed in rabbit proximal tubule cells. Similar to MAO-B in liver, this isoform possesses $I_2$BS accessible to the ligands. In intact cells, $I_2$BS ligands diffuse into the cells and bind to and inhibit MAO-B activity. The interaction of $I_2$BS ligands with MAO-B in intact cells further supports the interest in this class of molecules as potential MAO inhibitors *in vivo*.

## Materials and Methods

**Rabbit proximal tubule cell preparation.** Rabbit kidney proximal tubule cells were isolated from New Zealand White rabbits using the technique previously described by Poujeol and Vandewalle (23). For each experiment, one adult male rabbit (CPA, Olivet, France) was killed by intravenous injection of 5 ml of pentobarbital sodium (Leo, St. Quentin/Yveline, France) and 2500 units of heparin (Sanofi, Libourne, France). Then, kidneys were removed rapidly and perfused with RPMI-1640 medium (GIBCO BRL, Cergy Pontoise, France) devoid of sodium bicarbonate and L-glutamine and buffered with 25 mM HEPES at pH 7.4. After decapsulation, the superficial cortex of the kidney was sliced, rinsed, and, finally, homogenized in a Dounce homogenizer (pestel A) (Polylabo, Strasbourg, France). The homogenate was successively filtered through 100-, 40-, and 20 $\mu$M nylon meshes (Technofix, Arcueil, France) and centrifuged at 245 $\times$ *g* for 10 min. The resulting supernatant was discarded, and the pellet was resuspended in RPMI-1640 medium and centrifuged twice, once at 44 $\times$ *g* for 15 sec and once at 245 $\times$ *g* for 10 min. After the second centrifugation, the pellet containing the cells was resuspended in buffer A (10 mM Tris·HCl, 140 mM NaCl, 5 mM KCl and 5 mM glucose, pH 7.4). This procedure yielded from $2 \times 10^8$ to $3 \times 10^8$ cells. The total number of cells was estimated by microscopic observation, and cells were used at a final concentration of $4 \times 10^6$ cells/ml in buffer A.

**Mitochondrial membrane preparations from renal cortex.** Mitochondrial membranes were obtained as previously reported (24). Rabbit renal cortices were washed in ice-cold buffer B (250 mM sucrose, 0.1 mM phenylmethylsulfonyl fluoride, 2 mM Tris-HEPES, pH 7.4) and disrupted in a Turrax homogenizer (Jankel & Kunkel KG, Staufen, UK). After 10 additional passes in a Dounce homogenizer, the homogenate was filtered through two layers of cheesecloth mesh and centrifuged at 500 $\times$ *g* for 10 min at 4°. The resulting pellet was discarded, and the supernatant was centrifuged at 16,000 $\times$ *g* for 30 min at 4°. The supernatant and the white upper pellet of this centrifugation were eliminated. The intermediate pellet (mitochondrial fraction) was washed twice in ice-cold buffer containing 50 mM Tris·HCl, 2 mM EGTA, pH 7.4, and protease inhibitors (0.1 mM phenylmethylsulfonyl fluoride, 10 $\mu$g/ml bacitracin, and 2 $\mu$g/ml soybean trypsin inhibitor) and stored at −80°.

**[$^3$H]Idazoxan binding.** Isolated cells from rabbit kidney proximal tubules ($4 \times 10^6$ cells/ml) were incubated with [$^3$H]idazoxan at 4° for 70 min in a final volume of 500 $\mu$l of buffer A in the presence of $10^{-6}$ M rauwolscine to mask $\alpha_2$-adrenoceptors. Incubation was stopped by adding 5 ml of ice-cold buffer C (10 mM Tris·HCl and 140 mM NaCl, pH 7.4). Then, samples were filtered through glass fiber filters (Whatman, Maidstone, UK), washed with 2 $\times$ 5 ml of buffer C, and placed in 5 ml of Ready-Safe scintillation fluid (Beckman Instruments, Palo Alto, CA). Radioactivity was counted in a liquid scintillation spectrometer (Model Tri-Carb 4000; Packard, Meriden, CT) at 56% efficiency.

Nonspecific binding, which represents 30–35% of the total binding at radioligands concentrations around the dissociation constant ($K_d$) was defined in the presence of 10 $\mu$M cirazoline.

For radioligand binding assay in the supernatant of digitonin-treated cells, the incubation was stopped by precipitation with 1 mg/ml bovine $\gamma$ globulin (in 100 mM Tris·HCl, pH 7.4)/25% polyethylene glycol, followed by vacuum filtration over glass fiber filters (GF/B; Whatman). The filters were then washed with 2 $\times$ 4 ml of 8% polyethylene glycol in 50 mM Tris·HCl, pH 7.4 (24).

**MAO activity.** Renal cortical membranes or isolated cells (100–200 $\mu$g) were incubated at 37° for 20 min for a final volume of 250 $\mu$l of sodium phosphate buffer, 50 mM, pH 7.5, with the required concentrations of [$^{14}$C]tyramine, [$^{14}$C]5-HT, or [$^{14}$C]$\beta$-phenylethylamine. Clorgyline ($10^{-6}$ M) or deprenyl ($10^{-7}$ M) was used to define specific MAO-A or MAO-B activity, respectively. Inhibition curves in membrane preparations from rabbit renal cortex showed that these clorgyline and deprenyl concentrations selectively inhibited MAO-A and MAO-B activities (data not shown). The reaction was ended by adding 1 ml of HCl at 4°. The reaction product was extracted by adding 2 ml of ethyl acetate/toluene (v/v), and the radioactivity contained in the organic phase was counted in a liquid scintillation spectrometer at 97% efficiency.

**Cell viability.** Cell viability was determined by using the trypan blue exclusion test and the measure of the LDH released from the cells. LDH activity was determined by using an Enzyline LDH Standardisé 50 assay kit (Bio Mérieux, Charbonnières les Bains, France).

**Photoaffinity labeling.** The cirazoline derivative AZIPI was iodinated and converted to the photolabile azide ([$^{125}$I]AZIPI) for use as a photoaffinity adduct as described previously by Lanier *et al.* (25). Rabbit renal proximal tubule cells were first sonicated and then incubated in reduced light with 1–2 nM [$^{125}$I]AZIPI for 30 min at 24°, chilled on ice, and diluted 10-fold with a buffer containing 50 mM Tris·HCl, pH 7.4, 2 mM EGTA, 1 mM $MgCl_2$, and 2 mM dithiothreitol. Samples were immediately photolyzed at 4° for 5 min in a photolysis chamber (320 nm). Photolabeled membranes were centrifuged, solubilized in sample buffer (60 mM Tris·HCl, pH 6.8, 10% glycerol, 2% SDS, 1% 2-$\beta$-mercaptoethanol, and 0.05% bromphenol blue) at 100° for 5 min, and, finally, subjected to 9% SDS-PAGE. After electrophoresis, the gels were dried under a vacuum and analyzed using a 445 SI PhosphorImager (Molecular Dynamics, Sunnyvale, CA).

**Immunoblot.** Sonicated proximal tubule cells and renal cortex membranes were solubilized in the SDS-PAGE sample buffer. Two

hundred micrograms of protein per well were loaded onto 9% SDS-PAGE gels. Resolved proteins were electrophoretically transferred to polyvinylidene difluoride membranes by semidry electroblotting (*Trans*-Blot SD; BioRad, Richmond, CA), and blots were blocked with 5% nonfat dry milk in wash buffer (phosphate-buffered saline, pH 7.5, and 0.1% Tween 20), washed twice, and incubated for 1 hr at room temperature with rabbit polyclonal antisera to MAO-A and MAO-B. The polyclonal antisera were obtained from rabbits immunized with the peptide TNGGQERKFVGGSGQ, which corresponds to amino acids 210–227 in MAO-A and 202–217 in MAO-B. The specificity of the antibody was determined by peptide competition in heterologous expression systems and various tissues. After being washed, blots were incubated with peroxidase-labeled anti-rabbit IgG for 40 min. Bound antibodies were detected using enhanced chemiluminescence (Amersham Life Sciences, Clearbrook, IL) and exposure to Amersham Hyperfilm MP film.

**Statistics.** [$^3$H]Idazoxan binding and MAO steady state kinetic parameters were evaluated using a nonlinear least-squares curve-fitting procedure (Prism; GraphPad, San Diego, CA). Results are expressed as the mean ± standard deviation. The statistical comparison of the results was obtained by using the Student's unpaired *t* test.

**Drugs and Chemicals.** [$^3$H]Idazoxan (40–60 Ci/mmol) was obtained from Amersham International (Buckinghamshire, UK), and rauwolscine was obtained from Roth (Karlsruhe, Germany). Cirazoline was a gift from Synthélabo (Paris, France). Idazoxan and rilmenidine were supplied by I.R.I. Servier (Suresnes, France). All remaining drugs and chemicals were purchased from Sigma (Paris, France).

## Results

In a first series of experiments, the expression of MAO was investigated in the rabbit renal cortex. MAO isoforms were identified by Western blot analysis and enzyme assays. Western blot analyses were performed using an antiserum obtained for rabbits immunized with a peptide common to MAO-A and MAO-B and conserved in humans, rats, and calves. The specificity of this antiserum was defined by showing that 1) the apparent molecular masses of the two bands detected by this antiserum are identical to those of MAO-A and MAO-B, as determined by SDS-PAGE (approximately 60 and 55 kDa, respectively) (26); 2) in various tissues, the identification of the MAO isoforms by Western blot analysis or enzyme assays supplied identical results (data not shown); and 3) immunolabeling was prevented by the preincubation of the antiserum with the synthetic peptide. As shown in Fig. 1A, Western blot analysis of membrane preparations from renal cortex revealed two peptides with the apparent molecular weights expected for the two isoforms of MAO. The identification of these two peptides with MAO-A and MAO-B was confirmed by enzyme assays. Indeed, both [$^{14}$C]5-HT and [$^{14}$C]PEA, used as substrates for MAO-A and MAO-B, respectively, were degraded after incubation with membrane preparations from rabbit renal cortex (PEA, $V_{max}$ = 1.57 ± 0.31 nmol/min/mg protein; 5-HT, $V_{max}$ = 166 ± 21 pmol/min/mg protein). [$^{14}$C]5-HT oxidation was inhibited by the MAO-A inhibitor clorgyline but was unaffected by the MAO-B inhibitor deprenyl. In contrast, [$^{14}$C]PEA degradation was prevented by deprenyl but not by clorgyline (Fig. 1B). These data show that both MAO-A and MAO-B are expressed in rabbit renal cortex.

Next, we investigated whether the MAO activity in the renal cortex could be related to the localization of the enzyme in the proximal tubule. With this aim, Western blot analysis

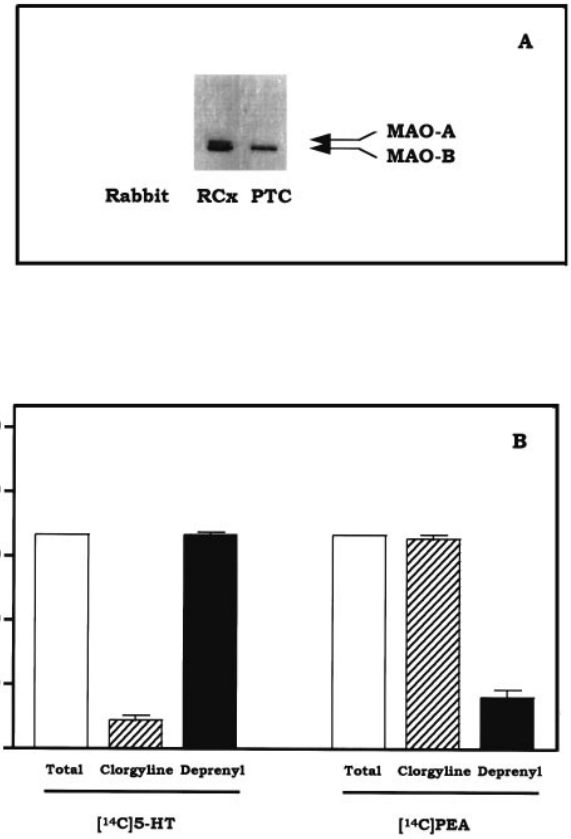


**Fig. 1.** A, Immunoblot of MAO-A and MAO-B in rabbit renal cortex (*RCx*) and in rabbit proximal tubule cells (*PTC*). Membranes from these tissues (200 μg) were electrophoresed on a 9% SDS-PAGE gel and transferred to polyvinylidene difluoride membranes. The blot was incubated with a rabbit polyclonal antiserum to both MAO isoforms. Immunoreactive proteins were identified as described in Materials and Methods. *Arrows,* migration of immunoreactive proteins with molecular masses of 60 and 55 kDa. B, MAO activity in rabbit renal cortex membranes (100–200 μg) using [$^{14}$C]PEA and [$^{14}$C]5-HT as substrates. Deprenyl ($10^{-7}$ M) and clorgyline ($10^{-6}$ M) were used to define specific MAO-B and MAO-A activities, respectively. Results are presented as the mean ± standard deviation of three independent experiments.

and enzyme assays were performed on isolated proximal tubule cells. Before enzyme assay, isolated cells were disrupted by sonication to make MAO-A and MAO-B fully accessible to their substrates. In contrast to the results obtained in renal cortex, only MAO-B could be detected by immunoblot in isolated proximal tubule cells (Fig. 1A). Enzyme assays showed that the MAO-B substrate [$^{14}$C]PEA was degraded in a dose-dependent manner after incubation with disrupted proximal tubule cells and had a $V_{max}$ similar to that found in the renal cortex ($V_{max}$ = 1.31 ± 0.41 nmol/min/mg protein, $K_m$ = 30.6 ± 8.2 μM, $n$ = 3). In contrast, oxidation of the MAO-A substrate [$^{14}$C]5-HT was only detectable and was significantly decreased with respect to the renal cortex ($V_{max}$ = 80.3 ± 19 pmol/min/mg protein, $K_m$ = 67 ± 18 μM, $n$ = 3, $p < 0.01$) (Fig. 2). These results indicate that MAO-B is the predominant MAO isoform expressed in the renal proximal tubule.

It has been previously shown that the accessibility of MAO-B $I_2$BS to their ligands may depend on the tissue localization. Indeed, the use of the photoaffinity $I_2$BS ligand [$^{125}$I]AZIPI allowed the photolabeling of human liver but not human platelet MAO-B (13). To verify whether renal proxi-

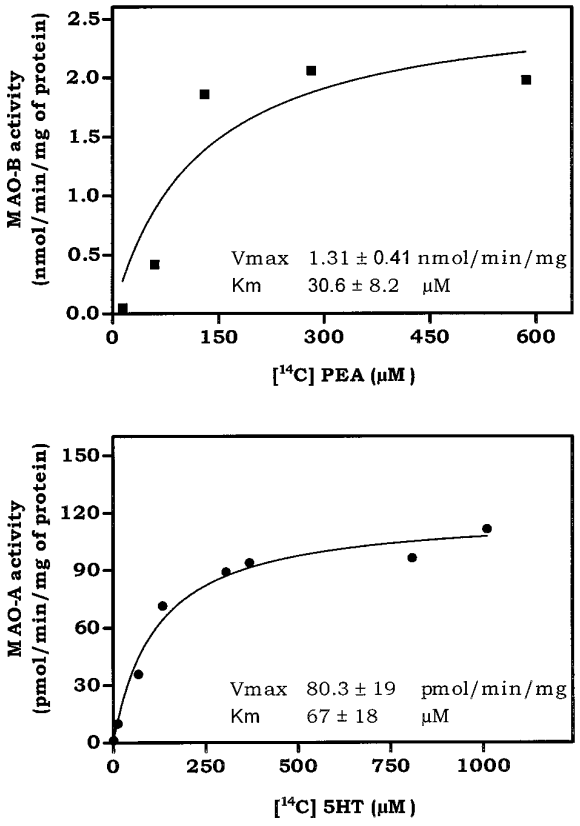


**Fig. 2.** Concentration-dependent oxidation of [$^{14}$C]PEA (upper panel) and [$^{14}$C]5-HT (lower panel) in rabbit proximal tubule isolated cells. The MAO-A–specific and MAO-B–specific activities were defined by using clorgyline ($10^{-6}$ M) and deprenyl ($10^{-7}$ M), respectively. This results shown in this figure are representative of three separate experiments.

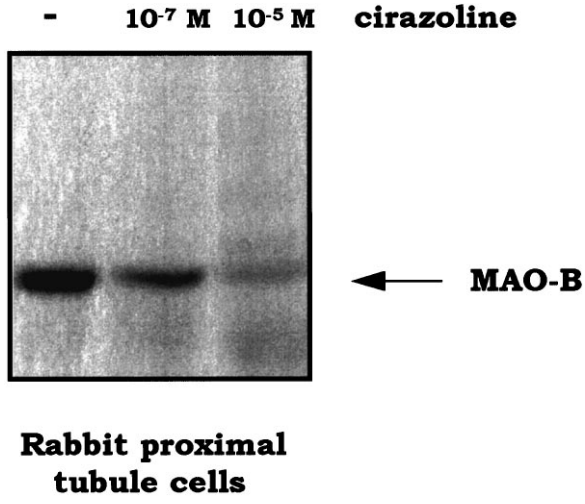


**Fig. 3.** Photoaffinity labeling of rabbit proximal tubule cells with the $I_2$-imidazoline ligand [$^{125}$I]AZIPI. Membranes from isolated cells (300 $\mu$g) were photolabeled with [$^{125}$I]AZIPI (1–2 nM) in the presence or absence of $10^{-7}$ or $10^{-5}$ M cirazoline. After SDS-PAGE, the gels were dried under a vacuum and analyzed using a Molecular Dynamics PhosphorImager. *Arrow,* migration of photolabeled protein with a molecular mass of 55 kDa.

mal tubule MAO-B holds the $I_2$BS, we performed photoaffinity labeling experiments in proximal tubule cells. As shown in Fig. 3, incubation of isolated cells with [$^{125}$I]AZIPI followed by SDS-PAGE revealed a single band with the apparent molecular weight identical to that of MAO-B. Blot exposure for up to 3 days in a Storage Phosphor Screen (Molecular Dynamics, Sunnyvale, CA) and detection with a Molecular Dynamic 445 SI PhosphorImager did not allow the identification of additional photolabeled bands.

To verify whether $I_2$BS ligands are able to enter the cell to bind to MAO-B, we performed [$^3$H]idazoxan binding studies and enzyme assays in isolated cells from rabbit proximal tubule. Binding studies were performed at 4° to attenuate a possible internalization of the ligand-receptor complex. [$^3$H]idazoxan-specific binding to intact cells was saturable and of high affinity (Fig. 4). Scatchard plot of saturation isotherms (Fig. 4, *inset*) was a linear function, which indicates that [$^3$H]idazoxan binds to an homogeneous population of high affinity sites with a maximal density of 848 ± 193 fmol/mg protein and an apparent $K_d$ of 4.7 ± 1.8 nM. In competition studies, [$^3$H]idazoxan-specific binding was fully inhibited by a series of imidazoline and guanidinium derivatives with an order of potency similar to that found in mitochondrial membrane preparations [guanabenz (1.9 ± 0.8 nM) > cirazoline (12 ± 9 nM) > idazoxan (22 ± 6 nM) > rauwolscine (> 10,000 nM)]. To define the intracellular component of radioligand binding, we first investigated the sensitivity of [$^3$H]idazoxan binding to proteases' treatment. Indeed, several studies have shown that, in intact cells, the binding of various radioligands to intracellular binding sites is resistant to treatment with proteases. Unfortunately, two major problems precluded the use of this technique for our purposes: 1) in preliminary experiments, performed in membrane preparations, we found that [$^3$H]idazoxan binding to $I_2$BS was extremely resistant to proteases' treatment, as elevated concentrations of trypsin, proteinase K, or pronase were required to induce only a partial binding inhibition; 2) such protease concentrations dramatically decreased the viability of renal proximal tubule cells.

As an alternative approach, we investigated whether [$^3$H]idazoxan binding to intracellular $I_2$BS required cell permeabilization. Therefore, intact cells were incubated with [$^3$H]idazoxan until the binding equilibrium was reached (70

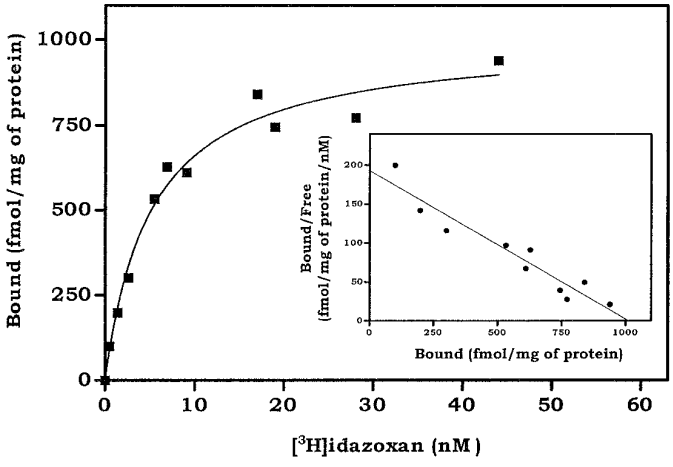


**Fig. 4.** Saturation analysis of [$^3$H]idazoxan-specific binding to rabbit proximal tubule cells. Cells were incubated with increasing concentrations of [$^3$H]idazoxan (1–50 nM) for 70 min at 4°. Cirazoline (10 $\mu$M) was used to define nonspecific binding, and rauwolscine $10^{-6}$ M was added to the incubation medium to mask $\alpha_2$-adrenoceptors. *Inset,* Scatchard plot of binding isotherms. This results shown in this figure are representative of five independent experiments.

min). Then, intracellular $I_2$BS were made fully accessible to the radioligand by cell permeabilization using the detergent digitonin. Finally, membrane-bound [$^3$H]idazoxan was separated from the free radioligand by filtration through glass fiber filters.

Cell release of the cytosolic enzyme LDH was used as an index of cell permeabilization. LDH activity was not detectable in the supernatant of isolated cells maintained at 4° for up to 120 min (data not shown). As shown in Fig. 5A, cell treatment with digitonin induced the release of LDH and, at the same time, decreased [$^3$H]idazoxan binding. The effect of digitonin was dose-dependent and reached the maximum at a concentration of 0.01%. [$^3$H]Idazoxan binding and LDH release were positively correlated ($p < 0.001$) (Fig. 5B). Two observations indicated that the decrease in [$^3$H]idazoxan binding was not related to the solubilization of membrane-bound $I_2$BS: 1) experiments performed in membrane preparations showed that solubilization of $I_2$BS required digitonin concentrations higher than 0.2% (24) and 2) no binding activity was detected in the cell supernatant as defined using

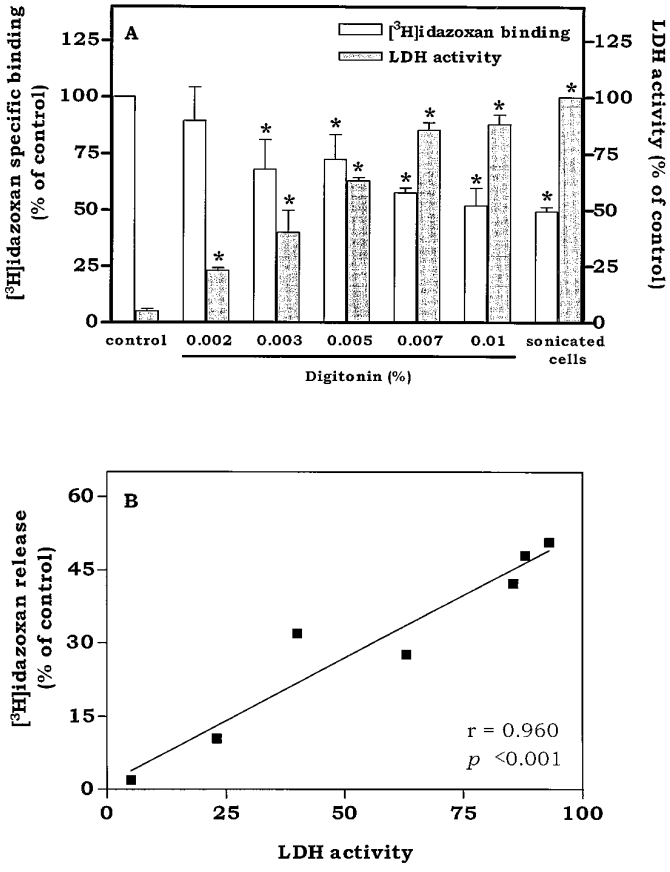


**Fig. 5.** A, Digitonin treatment effect on [$^3$H]idazoxan binding and LDH release in rabbit proximal tubule isolated cells. Cells were incubated with [$^3$H]idazoxan (8–10 nM) until the equilibrium state was reached (70 min). They were then treated with increasing digitonin concentrations for 5 min at 4°. Incubation was stopped by dilution with buffer C, and the free radioligand was separated from the bound radioligand by filtration. Samples were processed exactly as for the binding assay to measure LDH release. After digitonin treatment, samples were centrifuged, and the supernatant was collected for LDH assay. Results are presented as the mean ± standard deviation of six independent experiments. *, $p < 0.05$ compared with control. B, Correlation between [$^3$H]idazoxan and LDH releases from rabbit proximal tubule isolated cells after treatment with increasing digitonin concentrations.

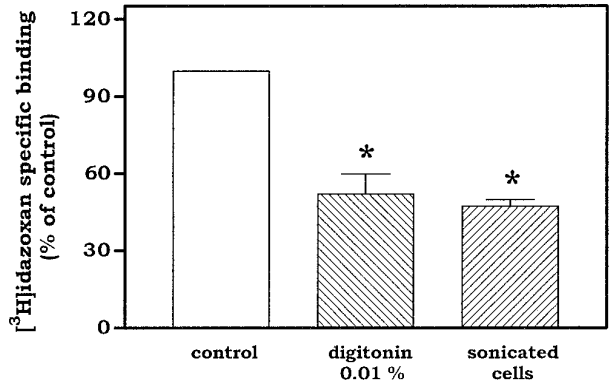


**Fig. 6.** [$^3$H]idazoxan-specific binding to rabbit proximal tubule isolated cells before and after digitonin (0.01%) treatment or cells sonication. Results are presented as the mean ± standard deviation of six independent experiments. *, $p < 0.001$ compared with control.

the filtration protocol for soluble proteins. As shown in Fig. 6, the residual [$^3$H]idazoxan binding found after cell treatment with 0.01% digitonin was similar to that determined in isolated cells sonicated before binding assay. These data indicate that, in intact cells, intracellular $I_2$BS are fully occupied by specific imidazoline and guanidinium ligands.

These results were confirmed by the experiments on the inhibition of MAO activity by imidazoline and guanidinium drugs performed in intact cells. Cells were incubated for 20 min with various imidazoline and guanidinium derivatives before the addition of the MAO substrate [$^{14}$C]tyramine. As shown in Fig. 7, MAO activity was inhibited by the $I_2$BS ligand cirazoline, guanabenz, and idazoxan and was not affected by the $I_2$BS ligands clonidine and rilmenidine. This order of potency is identical to that found in sonicated cells (data not shown) and corresponds to the pharmacological profile of $I_2$BS. Thus, both radioligand binding studies and enzyme assays clearly showed that, in intact cells, $I_2$BS ligands can bind to and inhibit MAO activity.

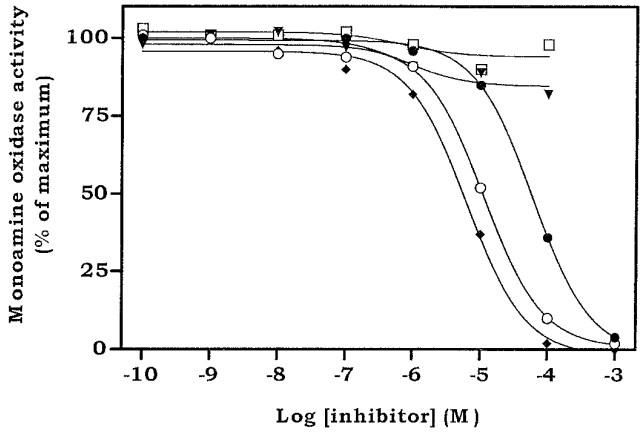


**Fig. 7.** Inhibition of MAO activity by imidazoline and related compounds. Isolated cells from rabbit proximal tubule ($4 \times 10^6$ cells/ml) were incubated in presence of increasing concentrations of cirazoline (◆), guanabenz (○), idazoxan (●), clonidine (□), and rilmenidine (▼) for 20 min. MAO-specific activity was measured in the presence of [$^{14}$C]tyramine at concentrations of approximately 200 μM. The results are representative of three to five separate experiments.

## Discussion

Noradrenaline and dopamine, two neurotransmitters metabolized by MAO, play a critical role in the regulation of sodium handling in the renal proximal tubule. In this segment of the nephron, these two catecholamines induce opposite effects: noradrenaline increases tubular sodium reabsorption by the activation of the $Na^+/H^+$ antiporter (27), whereas dopamine decreases tubular sodium reabsorption by regulating different transport systems, including the $Na^+/H^+$ antiporter, the $Na^+$-$K^+$ pump, and the $Na^+$/Pi cotransport (28, 29). Although noradrenaline is released by renal sympathetic nervous endings, most dopamine is directly synthesized by the renal proximal tubule cells. Indeed, it has been shown that the dopamine precursor L-dihydroxyphenylalanine is transported into the cells and is converted into dopamine by aromatic-L-amino acid decarboxylase (30). Dopamine is then secreted by the renal proximal tubule cells and acts as an autocrine/paracrine factor.

Recent studies have shown the extraneuronal location of both MAO-A and MAO-B in the renal tissues (31) and their involvement in the regulation of renal dopamine content. Indeed, experiments performed in rat renal cortical slices showed that inhibition of MAO increases the dopamine release and decreases the concentration of the dopamine metabolites dihydrophenylacetic acid and homovanillic acid (32). The study of the effect of selective MAO inhibitors on dopamine accumulation suggests that, at least in the rat, both MAO-A and MAO-B are responsible for degradation of renal dopamine. The identification of the MAO isoforms expressed in the proximal tubule represents a critical step in the comprehension of their respective roles in the metabolism of renal dopamine.

In the present study, we showed that both MAO-A and MAO-B are expressed in the rabbit renal cortex. In contrast, three major findings indicate that MAO-B is the predominant MAO isoform expressed in the rabbit renal proximal tubule: 1) Western blot analysis revealed a single 55-kDa band corresponding to MAO-B; 2) enzyme assays showed an elevated MAO-B activity, whereas MAO-A activity was only detectable; and 3) photoaffinity labeling with the $I_2$BS ligand [$^{125}$I]AZIPI revealed only MAO-B in isolated proximal tubule cells, whereas both MAO isoforms were detected in the rabbit renal cortex (26). Such localization of MAO-B does not seem to be unique to the rabbit, as we have recently found elevated MAO-B activity in rat renal proximal tubule.[1] These results suggest that MAO-B may be the MAO isoform that plays a major role in the degradation of the dopamine produced by renal proximal tubule cells.

Photoaffinity labeling experiments show that rabbit renal proximal tubule MAO-B carries the $I_2$BS. Radioligand binding data performed in membrane preparations from isolated cells using [$^3$H]Ro 19−6327, a MAO-B–specific ligand, showed a density of MAO-B molecules 5- to 6-fold higher than that of $I_2$BS (data not shown). This different stoichiometry is in agreement with previous results (33) and confirms that $I_2$BS are localized on a subpopulation of the enzyme. Radioligand binding studies and enzyme assays clearly showed that, in intact renal proximal tubule cells, $I_2$BS ligands reach the cell cytosol and interact with MAO-B. The following observations suggest that the entrance of $I_2$BS ligands into the cells does not require specific transport systems: 1) radioligand binding experiments were performed at 4° to minimize the activity of the energy-dependent transport systems as well as the internalization of ligand-receptor complexes; 2) the entry of $I_2$BS ligands into the cells did not require specific co-transported factors. Indeed, [$^3$H]idazoxan binding to intracellular binding was maximal using an incubation medium containing only Tris and the nondiffusible cation substitute *N*-methyl-D-glucamine (7); 3) as previously reported in mitochondrial membrane preparations, Scatchard plot of saturation binding data was linear, which indicates that [$^3$H]idazoxan interacts with a single population of binding sites. Thus, $I_2$BS ligands seem to freely cross the plasma membrane after a gradient concentration. This possibility is supported by the fact that these ligands are strongly lipophilic, presenting an octanol/water coefficient partition higher than unit.

As shown by the enzyme assay, the interaction of $I_2$BS ligands with MAO induced a dose-dependent inhibition of the enzyme activity. Comparison of these results with those obtained from radioligand studies show that inhibition constants of imidazoline derivatives were lower for [$^3$H]idazoxan binding to $I_2$BS than for MAO activities. In previous studies (12), we made the hypothesis that, in membrane preparations, this discrepancy could be related to the absence of an unknown regulatory cell factor, which is necessary to increase the potency of imidazoline ligands for the inhibition of enzyme activity. The fact that we have observed the same discrepancy in an intact cell system makes this hypothesis unlikely. At present, the relationship between the occupancy of $I_2$BS and the inhibition of the enzyme activity needs further investigation. It is possible that MAO inhibition by the imidazoline ligands is related to the interaction with a low affinity site localized on the entire population of MAO. The characterization of the functional activity of the high affinity $I_2$BS, which is localized on a subpopulation of the enzyme, requires the identification and the isolation of the MAO subtype. Nevertheless, the demonstration that imidazoline ligands inhibit MAO activity in intact cells reveals a novel mechanism of action of this class of drugs and may have relevance in the therapy of diseases in which MAO function is altered.

Our findings may have particular relevance to the field of hypertension. Indeed, it has been shown that, in a subpopulation of hypertensive patients (34) and in rat models of essential hypertension (35), the renal dopamine content was decreased with respect to the control subjects. In addition, modification of MAO activity has been reported in a rat model of spontaneous hypertension (5).

The demonstration that MAO-B is the predominant isoform expressed in the proximal tubule is a critical step in defining its role in the control of tubular function and in the development of hypertension. The fact that $I_2$BS ligands interact with MAO-B in intact renal proximal tubule cells suggests a potential role for these compounds in the pharmacological control of MAO activity *in vivo*.

**Acknowledgments**

The authors thank Dr. Cesura (F. Hoffman-LaRoche, Basel, Switzerland) for providing [$^3$H]Ro 19−6327.

[1] C. Ordener, N. Pizzinat, A. Parini, manuscript in preparation.

**References**


1. Weyler, W., Y.-P. P. Hsu, and X. O. Breakefield. Biochemistry and genetics of monoamine oxidase. *Pharmacol. Ther.* **47:**391–417 (1990).
2. Bach, A. W., N. C. Lan, D. L. Johnson, C. W. Abell, M. E. Bembenek, S. W. Kwan, P. H. Seeburg, and J. C. Shih. c-DNA cloning of human liver monoamine oxidase A and B. Molecular basis of differences in enzymatic properties. *Proc. Natl. Acad. Sci. USA* **85:**4934–4938 (1988).
3. Grimsby, J., K. Chen, L. J. Wang, N. C. Lan, and J. C. Shih. Human monoamine oxidase A and B genes exhibit identical exon-intron organization. *Proc. Natl. Acad. Sci. USA* **88:**3637–3641 (1991).
4. Youdim, M. B. H., and J. P. M. Finberg. New directions in monoamine oxidase A and B selective inhibitors and substrates. *Biochem. Pharmacol.* **41(2):**155–162 (1991).
5. Yasuhara, H., S. H. Parvez, K. Oguchi, M. Sandler, and T. Nagatsu, eds. *Monoamine Oxidase: Basic and Clinical Aspects*. VSP, Utrecht, The Netherlands (1993).
6. Brunner, H. G., M. Nelen, X. O. Breakefield, H. H. Ropers, and B. A. van Oost. Abnormal behavior associated with a point mutation in the structural gene for monoamine oxidase A. *Science (Washington D. C.)* **262:**578–580 (1993).
7. Cases, O., I. Seif, J. Grimsby, P. Gaspar, K. Chen, S. Pournin, U. Müller, M. Aguet, C. S. Babinet. Aggressive behavior and altered amounts of brain serotonin and norepinephrine in mice lacking MAOA. *Science (Washington D. C.)* **268:**1763–1766 (1995).
8. Jarman, J., V. Glover, M. Sandler, N. Turjanski, and G. Stern. Platelet monoamine oxidase B activity in Parkinson's disease: a re-evaluation. *J. Neural. Transm.* **5:**1–4 (1993).
9. Singer, T. P., N. Castagnoli, Jr., R. R. Ramsay, and A. J. Trevor. Biochemical events in the development of Parkinsonism induced by 1-methyl-4-phenyl-1,2,3,6-tetrahydropyridine. *J. Neurochem.* **49:**1–8 (1987).
10. Saura, J., J. M. Luque, A. M. Cesura, M. Da Prada, V. Chan-Palay, G. Huber, J. Löffler, and J. G. Richards. Increased monoamine oxidase B activity in plaque-associated astrocytes of Alzheimer brains revealed by quantitative enzyme radioautography. *Neuroscience* **62:**15–30 (1994).
11. Sparks, D. L., V. M. Woeltz, and W. R. Markesbery. Alterations in brain monoamine oxidase activity in aging, Alzheimer's disease, and Pick's disease. *Arch. Neurol.* **48:**718–721 (1991).
12. Tesson, F., I. Limon-Boulez, P. Urban, M. Puype, J. Vandekerckhove, I. Coupry, D. Pompon, and A. Parini. Localization of $I_2$-imidazoline binding sites on monoamine oxidases. *J. Biol. Chem.* **270:**9856–9861 (1995).
13. Raddatz, R., A. Parini, and S. M. Lanier. Imidazoline/guanidinium binding domains on monoamine oxidases: relationship to subtypes of imidazoline binding proteins and tissue-specific interaction of imidazoline ligands with monoamine oxidase B. *J. Biol. Chem.* **270:**27961–27968 (1995).
14. Limon-Boulez, I., F. Tesson, C. Gargalidis-Moudanos, and A. Parini. $I_2$ imidazoline binding sites: relationship with different monoamine oxidase domains and identification of histidine residues mediating ligand binding regulation by $H^+$. *J. Pharmacol. Exp. Ther.* **276:**359–364 (1996).
15. Carpéné, C., P. Collon, A. Remaury, A. Cordi, A. Hudson, D. Nutt, and M. Lafontan. Inhibition of amine oxidase activity by derivatives that recognize imidazoline $I_2$ sites. *J. Pharmacol. Exper. Ther.* **272:**681–688 (1995).
16. Fernandes, M. H., and P. Soares-da-Silva. Type A, B monoamine oxidase activities in the human and rat kidney. *Acta. Physiol. Scand.* **145:**363–367 (1992).
17. Bello-Reuss, E. Effect of catecholamines on fluid reabsorption by the isolated proximal convoluted tubule. *Am. J. Physiol.* **238:**F347–F352 (1980).
18. Siragy, H. M., R. A. Felder, N. L. Howel, R. L. Chevalier, M. J. Peach, and R. M. Carey. Evidence that intrarenal dopamine acts as a paracrine substance at the renal tubule. *Am. J. Physiol.* **257:**F469–F477 (1989).
19. Itskowitz, H. D., Y. H. Chen, and C. Stier, Jr. Reciprocal renal effects of dopamine and 5-hydroxytryptamine formed within the rat kidney. *Clin. Sci.* **75:**503–507 (1988).
20. Baines, A. D., and W. Chan. Production of urine free dopamine from dopa: a micropuncture study. *Life Sci* **26:**253–259 (1980).
21. Lee, M. R. Dopamine and the kidney. *Clin. Sci.* **62:**439–448 (1982).
22. Fernandes, M. H., and P. Soares-da-Silva. Role of monoamine oxidase A and B in the deamination of newly formed dopamine in the rat kidney. *J. Neural. Transm.* **32:**155–159 (1990).
23. Poujeol, P., and A. Vandewalle. Phosphate uptake by proximal cells isolated from rabbit kidney: role of dexamethasone. *Am. J. Physiol.* **249:**F461–F471 (1985).
24. Limon, I., I. Coupry, S. M. Lanier, and A. Parini. Purification and characterization of mitochondrial imidazoline-guanidinium receptive site from rabbit kidney. *J. Biol. Chem.* **267:**21645–21649 (1992).
25. Lanier, S. M., B. Ivkovic, I. Singh, J. L. Neumeyer, and V. Bakthavachalam. Visualization of multiple imidazoline/guanidinium receptive sites. *J. Biol. Chem.* **268:**16047–16051 (1993).
26. Lanier, B., R. Raddatz, V. Bakthavachalam, I. Coupry, J. L. Neumeyer, and S. M. Lanier. Structural and ligand recognition properties of imidazoline binding proteins in tissues of rat and rabbit. *Mol. Pharmacol.* **48:**703–710 (1995).
27. Nord, E. P., J. M. Howard, A. Hafezi, P. Maradeshagi, S. Vaystab, and P. A. Insel. *Alpha*-2 adrenergic agonists stimulate $Na^+/H^+$ antiport activity in the rabbit renal proximal tubule. *J. Clin. Invest.* **80:**1755–1762 (1987).
28. M. R. Lee. Dopamine and the kidney: ten years on. *Clin. Sci.* **84:**357–375 (1993).
29. Perrichot, R., A. Garcia-Ocana, S. Couette, E. Comoy, C. Amiel, and G. Friedlander. Locally formed dopamine modulates renal Na-Pi co-transport through $DA_1$ and $DA_2$ receptors. *Biochem. J.* **312:**433–437 (1995).
30. P. Soares-da-Silva. Enhanced protein kinase C mediated inhibition of renal dopamine synthesis during high sodium intake. *Biochem. Pharmacol.* **45:**1791–1800 (1993).
31. Caramona, M. M., and P. Soares-da-Silva. Evidence for an extraneuronal location of monoamine oxidase in renal tissues. *Naunyn-Schmiedeberg's Arch. Pharmacol.* **341:**411–413 (1990).
32. Fernandes, M. H., and P. Soares-da-Silva. Role of monoamine oxidase and catechol-*O*-methyltransferase in the metabolism of renal dopamine. *J. Neural. Transm.* **41:**101–105 (1994).
33. Sastre, M., and J. A. Garcia-Sevilla. Opposite age-dependent changes of $\alpha_{2A}$-adrenoceptors and nonadrenoceptors [$^3$H]idazoxan binding sites ($I_2$-imidazoline binding sites) in the human brain: strong correlation of $I_2$ with monoamine oxidase-B sites. *J. Neurochem.* **61:**881–889 (1993).
34. Sowers, J. R., M. B. Zemel, P. Zemel, F. W. J. Beck, M. F. Walsh, and E. T. Zawada. Salt sensitivity in Blacks: salt intake and natriuretic substances. *Hypertension (Dallas)* **12:**485–490 (1988).
35. De Feo, M. L., A. L. Jadhav, and M. F. Lokhandwala. Dietary sodium intake and urinary dopamine and sodium excretion during the course of blood pressure development in Dahl rats sensitive and salt resistant rats. *Clin. Exp. Hypertens. A* **9:**76–80 (1987).


**Send reprint requests to:** Angelo Parini, M.D., Ph.D., INSERM U388, CHU Rangueil, Institut Louis Bugnard, 31054 Toulouse Cedex, France. E-mail: parini@inserm.rangueil.fr